CHEMIJA. 2017. Vol. 28. No. 4. P. 206–213

Platinum/titania nanotube arrays as electrocatalysts for borohydride oxidation

Dijana Šimkūnaitė*,

Loreta Tamašauskaitė-Tamašiūnaitė,

Aldona Balčiūnaitė,

Aušrinė Zabielaitė,

Sigitas Jankauskas,

Algirdas Selskis

State Research Institute,
Center for Physical Sciences and Technology,
Saulėtekio Ave. 3,
10257 Vilnius, Lithuania

This work is focused on the study of Pt nanoparticles coated self-ordered titania nanotube arrayed electrodes (denoted as Pt/TiO_2-NTs) as efficient platinum/titania nanotubes electrocatalysts for the oxidation of sodium borohydride in an alkaline medium. The Pt/TiO_2-NTs catalysts with different Pt loadings were fabricated on the titania nanotubes arrayed surface via a facile electrochemical deposition technique. The surface morphology and composition of the Pt/TiO_2-NTs catalysts were investigated using field-emission scanning electron microscopy and energy dispersive X-ray spectroscopy. The electrochemical behaviour of the prepared catalysts was examined towards the oxidation of BH_4^- ions in an alkaline medium by means of cyclic voltammetry. It has been determined that the electrocatalytic activity of Pt/TiO_2-NTs catalysts towards the oxidation of BH_4^- ions depends on the Pt loading in the catalysts and is higher as compared with that of a smooth Pt electrode. It has been found that the Pt/TiO_2-NTs catalyst with a Pt loading of 16.3 $\mu g_{Pt}\,cm^{-2}$ and with deposited Pt nanoparticles ranging from several to 50 nm in size exhibited the highest specific and mass activities for the oxidation reaction of sodium borohydride.

Keywords: platinum, titania nanotubes, sodium borohydride, oxidation

INTRODUCTION

Sodium borohydride is regarded as a greatly promising fuel for fuel cells [1–3], especially for possible applications in portable electronic devices [2, 4, 5]. For that reason great scientific interest lies in the investigation of the sodium borohydride oxidation reaction (BOR) with an ultimate goal to identify the best conditions for its optimal performance. Development of perfect catalysts capable of promoting BOR has been the focus of much research recently. However, the best catalysts used in direct borohydride fuel cells (DBFCs) are still the noble ones. Commercial employment of these catalysts is hindered by the high costs of the main constitutive material of the electrode, since it significantly increases the total price of the fuel cell devices. The problem could be handled by employing single-, double- and multiple-component catalysts containing non-precious transition metals such as Ni, Co, Fe and Zn and further on fixing them on a new catalyst supports with preferential properties. Bi-metallic or multi-metallic systems with non-precious transition metals, including Au–Cu [6], Au–Co [7–9], Au–Fe [10], Au–Ni [11–13], Au–Zn [14], Ag–Cu [15], Pt–Cu [16], Pt–Co [17–19], Pt–Ni [19], Pt–Zn [20], Pd–Zn [21]], Au/Co/Cu [8], Cu–Ni–AuNi [22] etc., exhibit a considerably higher electrocatalytic activity and stability towards the oxidation of BH_4^- ions as compared to those of pure Au, Pt, Pd and Ag metals. The introduction of a secondary metal into the system allows both to reduce the cost of the catalyst and simultaneously to improve its catalytic characteristics towards oxidation of borohydride.

* Corresponding author. Email: dijana.simkunaite@ftmc.lt

On the other hand, in order to minimize the amount of the precious metal used and to increase the surface area for the reaction, the selection of a technologically relevant support becomes a focal point in advancing the application of DBFCs. It provides the possibility to maintain or even improve the reactivity of the electrocatalyst used decreasing the amount of the precious metal applied. On that ground, a variety of nanostructured conducting materials like the mesoporous ones, nanotubes or nanofibers were used as supports for Pt catalysts. One-dimensional catalyst supports, such as titanium oxide nanowires, nanoribbons, nanotubes and nanorods [23–25], have attracted a considerable attention recently. Titania nanotube arrays (denoted as TiO_2-NTs) have been successfully used as a substrate for loading the metal nanoparticles to create high performance catalysts, as they are readily prepared, highly oriented, provide a large surface area, are uniform, non-toxic, chemically stable, show an excellent electronic conductivity, a good corrosion resistivity and have low production costs [26–28]. TiO_2-NTs supports outperform carbon-based ones as the latter undergo oxidation/corrosion, especially in the presence of Pt [29]. Corrosion of carbon leads to Pt agglomeration, in consequence the electrochemically active catalyst surface area is reduced and electronic continuity in the catalyst layer is lost, performance degradation is evidenced. For those reasons, among the other supporting materials used, TiO_2-NTs could be differentiated as an attractive choice for the fabrication of high performance catalysts in fuel cells optimization.

Based on the aforementioned reasons, in this work we made an attempt to fabricate platinum/titania nanotubes electrocatalysts (denoted as Pt/TiO_2-NTs) for the oxidation of borohydride in an alkaline medium since they provide the possibility to increase the surface area for the reaction and to minimize the amount of precious metal used. Moreover, no data are present on using Pt/TiO_2-NTs to oxidize borohydride, nevertheless, platinum-coated nickel films (Pt/Ni) on the titania nanotubed electrodes have been fabricated and studied [31]. In this work well-adherent platinum-coated titania nanotubed electrodes (TiO_2-NTs) have been prepared via a simple electrochemical Pt deposition technique. The morphology, structure and composition of the prepared nanostructured catalysts were examined by field emission scanning electron microscopy (FESEM) and energy dispersive X-ray analysis (EDX) while their electrocatalytic activity towards the oxidation of borohydride ions in an alkaline medium was investigated by means of cyclic voltammetry.

EXPERIMENTAL

Chemicals

Ti foil of 99.7% purity, 0.127 mm in thickness, H_2PtCl_6 and $NaBH_4$ were purchased from Sigma-Aldrich Supply. HCl, NH_4F, H_2SO_4 NaOH and ethanol were purchased from Chempur Company. All chemicals were of analytical grade. Deionized water with the resistivity of 18.2 MΩ cm^{-1} was used to prepare all the solutions.

Fabrication of catalysts

Self-ordered TiO_2 nanotube arrays were formed onto the Ti substrates by means of anodic oxidation [12]. Briefly, prior to anodization, the 1 × 1 cm^2 titanium sheets were degreased with ethanol, rinsed with deionized water and dried in an Ar stream. The titanium sheets were anodized in a 0.24 M H_2SO_4 solution containing 0.5 wt.% NH_4F at a constant potential of 20 V and room temperature for 1 h. The counter electrodes were two sheets of Pt (99.99% purity). After anodization, the samples were rinsed thoroughly with deionized water and dried.

The Pt/TiO_2-NTs electrodes were fabricated by direct electroplating of Pt on the TiO_2 nanotubes by the electrochemical deposition technique in a 1 mM H_2PtCl_6 + 0.1 M HCl solution at 25°C by applying the cathodic current (i) of 10 mA cm^{-2} for 3, 15 and 30 min. The fabricated catalysts were used for sodium borohydride electro-oxidation measurements without any further treatment.

Characterization of catalysts

The morphology and composition of the fabricated catalysts were characterized using a SEM/FIB workstation Helios Nanolab 650 with an energy dispersive X-ray (EDX) spectrometer INCA Energy 350 X-Max 20. Pt metal loading was estimated using the STRATAGEM software and EDS K-ratios for Ni, P, Ti and O K alpha lines and Pt L alpha lines.

Electrochemical measurements

Electrochemical measurements were carried out in a conventional three-electrode cell containing 1 M NaOH and 0.05 M $NaBH_4$ at 25 ± 1°C. The prepared Pt/TiO_2-NTs catalysts served as a working electrode and a Pt sheet was used as a counter electrode. Electrode potentials (E) were measured in reference to the Ag/AgCl/KCl(sat) electrode from the stationary E_s value up to 0.6 V, at a potential scan rate of 10 mV s^{-1} and 25°C temperature. In some cases a Pt sheet of 2 cm^2 area was used as a pure smooth platinum electrode. The presented current densities are normalized with respect to the geometric area of catalysts.

The electrochemically active surface areas (ECSAs) of the prepared catalysts were determined from the cyclic voltammograms (CVs) of the Pt and Pt/TiO_2-NTs catalysts recorded in a deaerated 0.5 M H_2SO_4 solution at a scan rate of 50 mV s^{-1} by calculating the charge associated with hydrogen adsorption (210 μC cm^{-2}) [30].

All electrochemical measurements were recorded with a Metrohm Autolab potentiostat (PGSTAT100) using the Electrochemical Software (Nova 1.6.013).

RESULTS AND DISCUSSION

Physical characterization

In all the cases nanostructured Pt catalysts were supported on TiO_2-NTs arrays prepared by anodic oxidation of the Ti surface in an aqueous sulfuric acid solution containing some NH_4F. To get morphological information of the prepared

nanostructured catalysts FESEM was performed. A typical FESEM image of the self-ordered TiO_2-NTs support applied for catalyst fabrication is presented in Fig. 1a. The approximated average inner tube diameter corresponds to ca. 100 nm in length while the thickness of titania layers is developed to ca. 350 nm [12]. Representative FESEM images of Pt nanoparticles settled directly onto TiO_2-NTs via the electrochemical deposition technique ranging from a few to several tens and even hundreds nm in size are presented in Fig. 1b, c. Electroplating of Pt crystallites onto the TiO_2 nanotubes was performed in a 1 mM H_2PtCl_6 + 0.1 M HCl solution by applying a cathodic current of 10 mA cm^{-2} for different time periods lasting from 3 to 30 min. Uniform and well dispersed 10–50 nm sized Pt crystallites located at the rims and inside of TiO_2-NTs can be clearly observed after 3 min exposure to the cathodic current of 10 mA cm^{-2} (Fig. 1b). The significantly enhanced number of Pt nanoparticles shown in Fig. 1c still follows the contours of TiO_2-NTs and align themselves along the boundary of NTs walls even at a lengthy deposition time for 30 min although some of the platinum particles tend to agglomerate creating a large formation of several hundred nanometers in size.

The energy dispersive X-ray (EDX) results of the as-prepared catalysts depending on their preparation time are listed in Table 1. They clearly show that Pt, Ti and O are the main elements available in the sample, confirming the presence of Pt deposited on TiO_2-NTs. A high content of oxygen points to the occurrence of oxides precipitated during deposition and/or formed during sample exposure to air before EDX measurements. It should be mentioned that EDX measurements can be influenced at least partially by oxygen, since we cannot exclude the oxidation by air during the sample transfer. From the EDX results it clearly follows that increasing the Pt deposition time from 3 to 30 min the amount of Pt in the sample consistently grows.

Table 1. **Surface atomic composition of the Pt/TiO_2-NTs catalysts obtained depending on their preparation time by EDX analysis**

Pt deposition time, t_{dep}/min	All results in at. %		
	O	Ti	Pt
3	54.78	44.82	0.40
15	48.67	47.49	4.14
30	34.46	45.23	20.26

It has been determined that the Pt loadings were 16.3, 88.9 and 219.0 μg_{Pt} cm^{-2} in the as-prepared Pt/TiO_2-NTs catalysts after direct electroplating of the TiO_2-NTs surfaces in a platinum-containing solution for 3, 15 and 30 min, respectively.

Electrochemical characterization

The electrochemically active surface areas (ECSAs) of polycrystalline Pt and Pt in the synthesized Pt/TiO_2-NTs

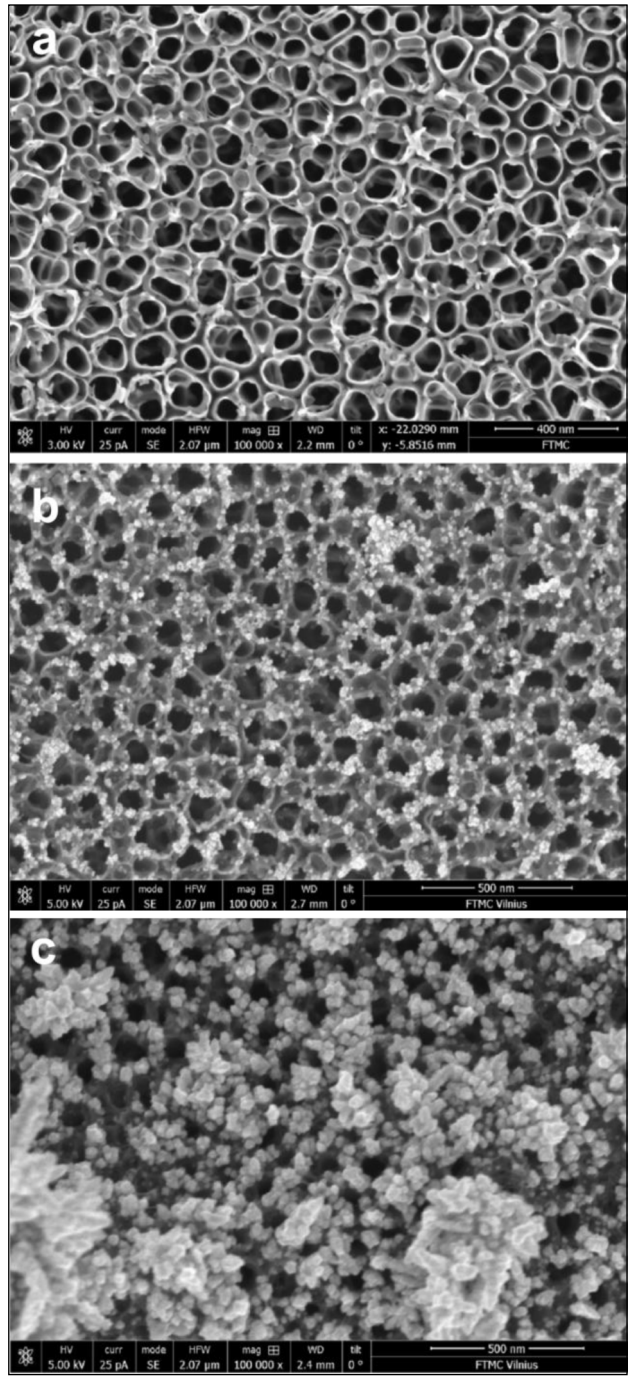

Fig. 1. FESEM images of TiO_2-NTs (a) and Pt/TiO_2-NTs (b, c) electrodes. The TiO_2-NTs arrays were prepared by anodic oxidation of Ti in 0.24 M H_2SO_4 and 0.5 wt.% NH_4F at a potential of 20 V for 1 h. The Pt/TiO_2-NTs catalysts were prepared by direct electroplating of Pt onto the TiO_2-NTs in a 1 mM H_2PtCl_6 + 0.1 M HCl solution at a current density of 10 mA cm^{-2} for 3 (b) and 30 min (c)

catalysts prepared by applying different deposition time periods (t_{dep}) of Pt onto TiO_2-NTs in a platinum containing solution were determined from the cyclic voltammograms of Pt and Pt/TiO_2-NTs catalysts recorded in a de-aerated 0.5 M H_2SO_4 solution at a sweep rate of 50 mV s^{-1} by calculating the charge associated with hydrogen adsorption (210 µC cm^{-2}) (Fig. 2) [30]. For a careful H_{upd}

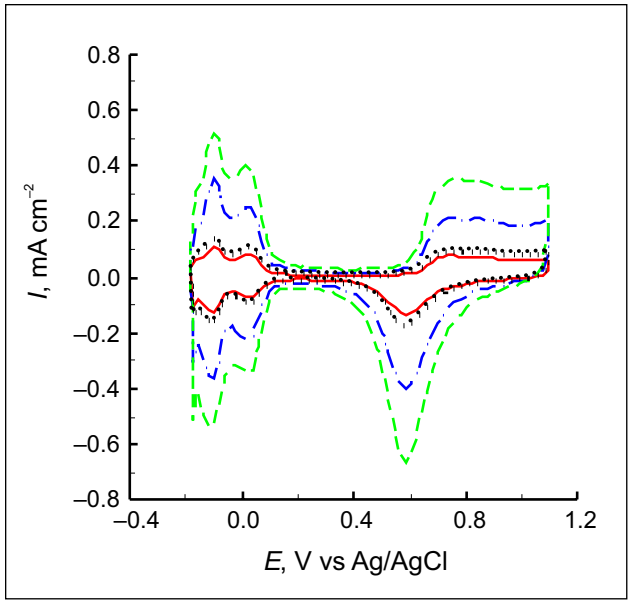

Fig. 2. CVs of Pt (a dotted line) and Pt/TiO_2-NTs catalysts in a deaerated 0.5 M H_2SO_4 solution at a scan rate of 50 mV s^{-1}. The Pt/TiO_2-NTs catalysts were prepared by direct electroplating of Pt onto TiO_2-NTs in a 1 mM H_2PtCl_6 + 0.1 M HCl solution at a current density of 10 mA cm^{-2} for 3 (a solid line), 15 (a dash-dotted line) and 30 min (a dashed line)

analysis, the capacitive currents from the double layer region were extrapolated into the potential region 0.2 V vs Ag/AgCl and taken as a subtraction baseline for the hydrogen adsorption/desorption peaks (to H_{upd} area correction). The lower potential limit for the integration of the charges was restricted by the minimum of the cathodic current before the onset of hydrogen evolution. The calculated hydrogen adsorption charges are 467.2 μC cm^{-2} for the polycrystalline smooth Pt and 356.3, 1092.4 and 1760.7 μC cm^{-2} for the Pt/TiO_2-NTs catalysts prepared by applying a cathodic current for 3, 15 and 30 min, respectively. The roughness factors for the same catalysts are 2.2, 1.7, 5.2 and 8.4. The estimated $ECSAs_{ads}$ values are 4.4 cm^{-2} for the smooth Pt and 3.4, 10.4 and 16.8 cm^{-2} for the Pt/TiO_2-NTs catalysts, respectively. Since the ECSAs values obtained from the hydrogen adsorption in the cathodic scan must agree with those obtained from the hydrogen desorption in the anodic scan we have performed the calculation of ECSAs values from the hydrogen desorption in the anodic scan. After the correction for the capacitive currents from the double layer region, the $ECSAs_{des}$ values obtained from the hydrogen desorption were 4.2 cm^{-2} for the smooth Pt and 3.3, 10.4 and 16.7 cm^{-2} for the Pt/TiO_2-NTs catalysts synthesized by direct electroplating of Pt onto TiO_2-NTs for different t_{dep}, i.e. 3, 15 and 30 min, respectively. We found the ratio of $ECSAs_{ads}/ECSAs_{des}$ = (1.03 ± 0.04). These results show that the ECSAs values of the Pt/TiO_2-NTs catalysts obtained after 15 and 30 min deposition of Pt onto TiO_2-NTs are ca. 2.4 and 3.8 times higher than that of the smooth Pt. Meanwhile, the ECSA value for the Pt/TiO_2-NTs catalyst, prepared by applying the cathodic current in the platinum-containing solution for t_{dep} = 3 min, is rather close to that of the smooth Pt, but it still remains 1.3 times lower than that of the smooth Pt.

The activity of the Pt/TiO_2-NTs catalysts, prepared by applying different deposition time periods of Pt onto TiO_2-NTs in the platinum containing solution, was investigated towards the oxidation of BH_4^- ions in an alkaline medium by the cyclic voltammetry technique. Figure 3a represents the behaviour of the TiO_2-NTs arrays in 0.05 M $NaBH_4$ + 1 M NaOH (a solid line), and in 1 M NaOH (a dotted line) solutions. The electrochemical oxidation processes of borohydride onto the smooth Pt (a dotted line) and Pt/TiO_2-NTs catalysts prepared by applying Pt deposition time for 3 (a solid line), 15 (a dash-dotted line) and 30 min (a dashed line) at a potential scan rate of 10 mV s^{-1} are presented in Fig. 3b. The oxidation process of BH_4^- ions on TiO_2-NTs verified with respect to that on the smooth Pt or the Pt/TiO_2-NTs catalysts is rather negligible and may be left out of consideration. The CVs for Pt supported onto the TiO_2-NTs array are not clearly pronounced but they follow the shape of that for the polycrystalline Pt and quite well reflect it at higher t_{dep} applied. Analogous shapes of CVs for Pt/TiO_2-NTs were observed in Ref. [31]. The voltammetric data for the polycrystalline Pt electrode, as well as these reported in Refs. [32–34], show that the voltammograms do not undergo radical transformations and are similar in shape. CV curves are typically associated with four characteristic oxidation peaks, i.e. two on the positive-going sweep and another two on the negative-going sweep labelled as **a1**, **a2**, **c1** and **c2**, respectively. The anodic peak **a1** at lower potential values may be related to the oxidation of H_2 generated by spontaneous hydrolysis of BH_4^-:

$$BH_4^- + H_2O \longrightarrow BH_3OH^- + H_2, \quad (1)$$

$$H_2 + 2\,OH^- \longrightarrow 2H_2O + 2\,e^-. \quad (2)$$

Another intermediate BH_3OH^-, produced by reaction (1), is also supposed to be capable of subsequent oxidation [35–37] by the reactions:

$$BH_3OH^- + 3\,OH^- \longrightarrow BO_2^- + 3/2\,H_2 + 2\,H_2O + 3\,e^- \quad (3)$$

or

$$BH_3OH^- + 6\,OH^- \longrightarrow BO_2^- + 5\,H_2 + 2\,H_2O + 6\,e^-. \quad (4)$$

The overall reaction of BH_4^- ion oxidation on Pt has been determined to proceed [38–41] through the four-electron process:

$$BH_4^- + 4\,OH^- \longrightarrow BO_2^- + 2\,H_2 + 2\,H_2O + 4\,e^-. \quad (5)$$

The second anodic oxidation wave **a2** at higher potentials, i.e. between 0 and 0.2 V, is attributed to the direct BH_4^- oxidation pathway with 5 or 6 e^- involved [33, 34]. In the reverse potential sweep, peak **c2** observed at about 0.3 V can be

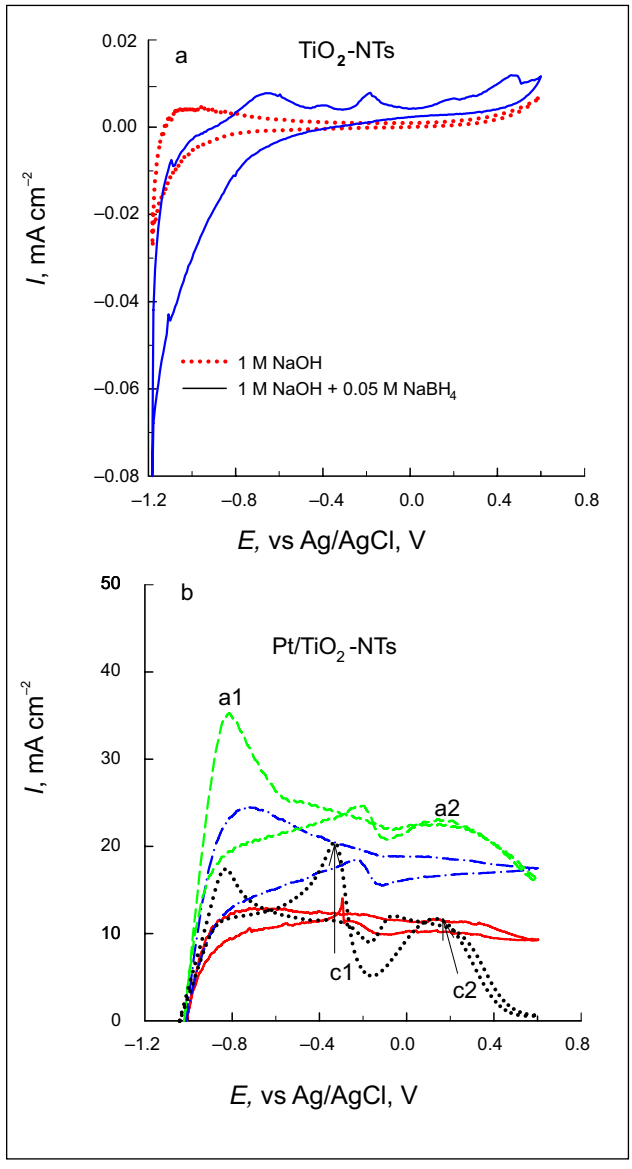

Fig. 3. (a) CVs of TiO_2-NTs in 1 M NaOH (a dotted line) and in 1 M NaOH + 0.05 M $NaBH_4$ (a solid line). (b) CVs of Pt/TiO_2-NTs catalysts prepared by direct electroplating of Pt onto TiO_2-NTs for 3 (a solid line), 15 (a dash-dotted line) and 30 min (a dashed line) in 1 M NaOH + 0.05 M $NaBH_4$. Potential sweep rate 10 mV s^{-1}, $T = 25$°C

assigned to the oxidation of absorbed intermediate oxidation products of BH_3OH^- on the partially oxidized Pt surface [33]. In the cathodic potential sweep wave **c2** corresponds to BH_4^- oxidation and is associated with the removal of Pt surface hydroxides or oxides in the dip of the CV curve at ca. –0.15 V, while peak **c1** corresponds to the oxidation of the $BH_3OH^-_{ad}$'s surface-adsorbed oxidation product [32]. In Ref. [34] peaks **c1** and **c2** were attributed to oxidation of intermediates, such as BH_2OH_{ad} and BOH_{ad}, respectively.

The current densities of borohydride oxidation recorded on the Pt/TiO_2-NTs catalysts prepared by direct electroplating of Pt onto TiO_2-NTs for 15 and 30 min are ca. 1.5 and 2 times higher than that on the pure Pt, meanwhile the current density on the Pt/TiO_2-NTs catalysts with t_{dep} = 3 min is almost the same as that on the smooth Pt. As was shown in Fig. 1 b and c, the increase in the Pt loading in the Pt/TiO_2-NTs catalysts results in a significantly enhanced number of Pt nanoparticles and the formation of larger structures developed to about several hundred nm in size. Such structures provide more absorption sites for involved molecules in a limited space, and allow faster electron transmission, which is favourable for the enhancement of Pt electrocatalytic properties [42]. Consequently, the enhancement of borohydride oxidation current is observed.

The borohydride oxidation current densities for the all synthesized Pt/TiO_2-NTs catalysts are stabilized with long-term

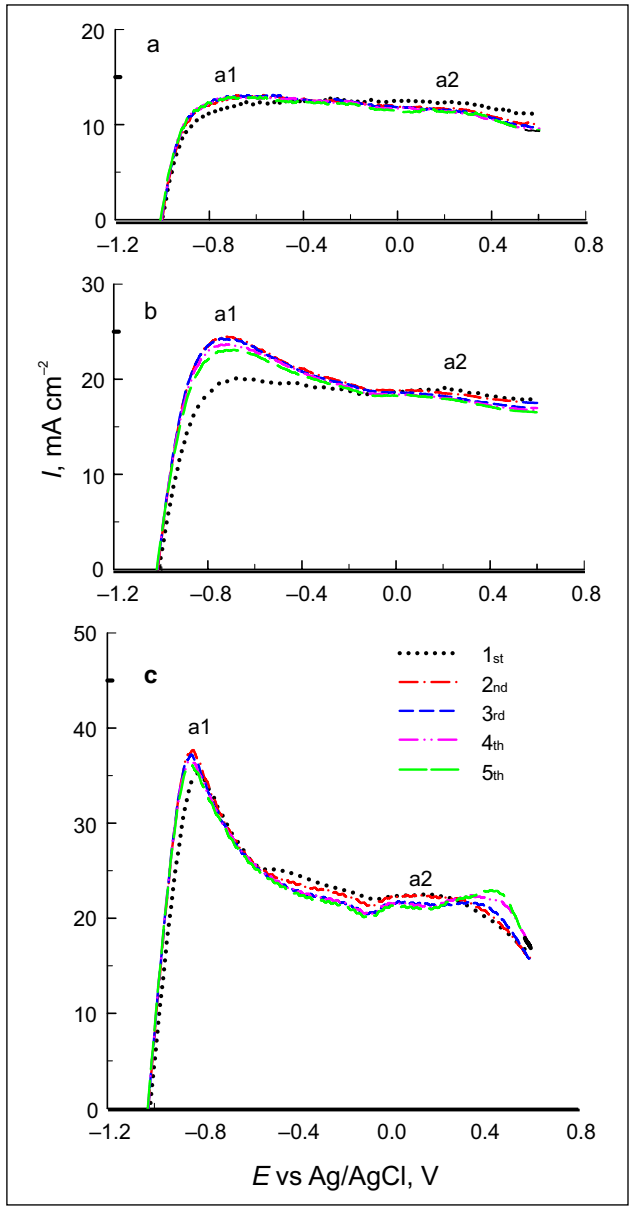

Fig. 4. Continuous CVs of the Pt/TiO_2-NTs catalysts with the Pt loadings of 16.3 (a), 88.0 (b) and 219.0 (c) μg cm^{-2} recorded in a 1 M NaOH + 0.05 M $NaBH_4$ solution at a potential scan rate of 10 mV s^{-1}, at 25°C. The number of scans: 1st is a dotted line, 2nd is a dash-dotted line, 3rd is a dashed line, 4th is a dash-dotted line and 5th is a long-dashed line

cycling and are shown in Fig. 44a–c. To facilitate the analysis of the CV curves only anodic going scans for different synthesis times of the catalysts are presented. The data obtained indicate a good efficiency of the studied catalysts and show the absence of any significant catalyst losses during the borohydride oxidation process.

To compare the electrocatalytic activity of the prepared catalysts, and to evaluate their specific (SA) and mass (MA) activities, the sodium borohydride oxidation current densities of the investigated catalysts were normalized by the electrochemically active surface areas and Pt loadings for each catalyst and are given in Fig. 5. It should be noted

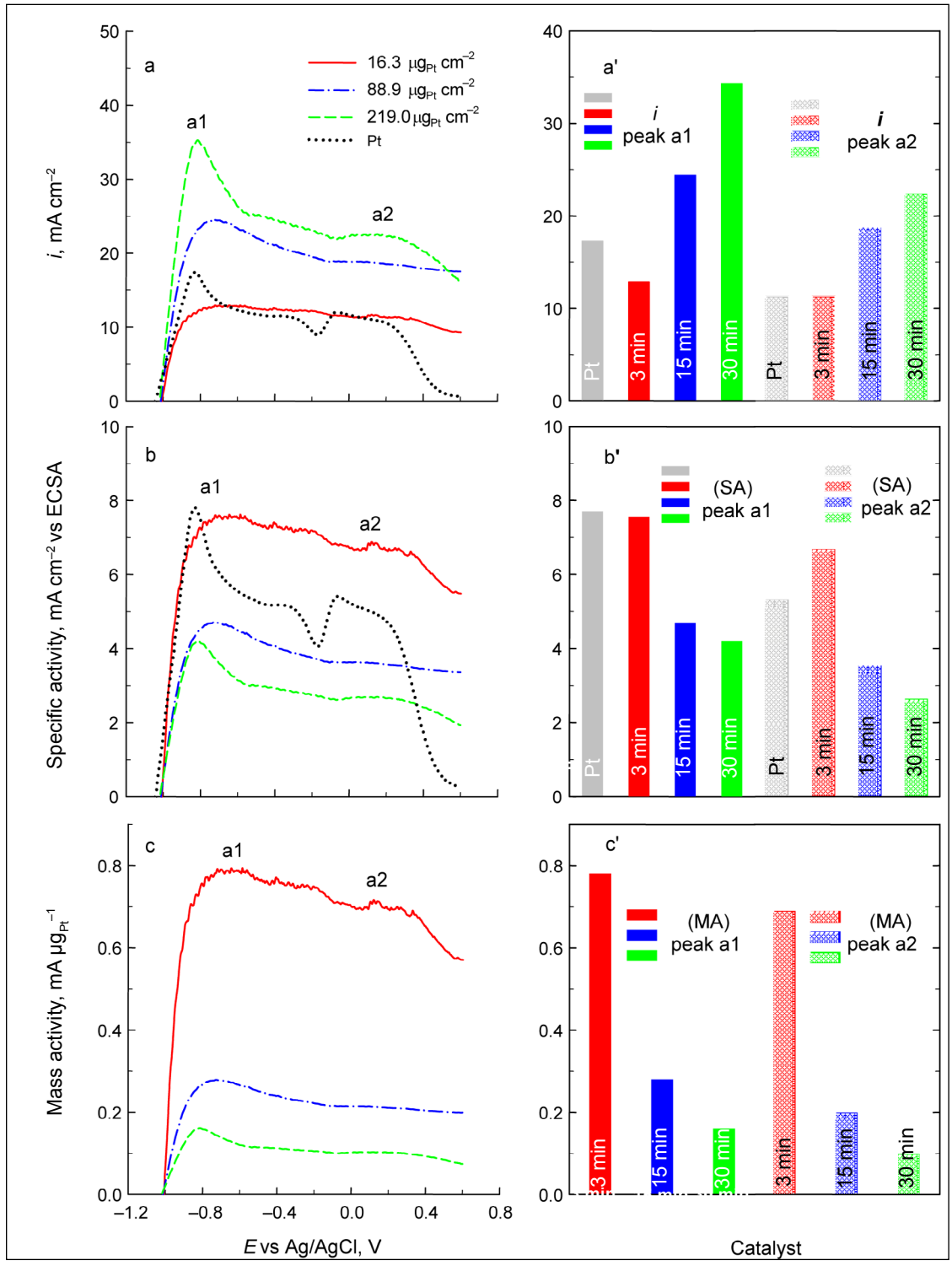

Fig. 5. (a) Positive going scans of BH_4^- ion oxidation recorded on the same catalysts as in Fig. 3. The same data normalized by the electrochemically active surface areas (b) and by the Pt loadings (c) in a 1 M NaOH + 0.05 M $NaBH_4$ solution at a potential sweep rate of 10 mV s^{-1}, 25°C; (a') comparison of current density; (b') specific activity; (c') mass activity values under peaks **a1** and **a2** for Pt and Pt/TiO_2-NT catalysts as in (a), (b) and (c)

that in spite of a ca. 1.3 times higher active surface area of the smooth Pt electrode compared to that of the Pt/TiO_2-NTs catalyst with the Pt loading of 16.3 μg_{Pt} cm^{-2}, the surface area normalized borohydride oxidation current under peak **a2** is ca. 1.3 times higher on the nanostructured catalyst (Fig. 5b, b'). Nevertheless, the ECSAs for the Pt/TiO_2-NTs catalysts with the Pt loadings of 88.9 and 219.0 μg_{Pt} cm^{-2} are ca. 3 and 5 times higher, respectively, compared to that of the Pt/TiO_2-NTs catalyst with the Pt loading of 16.3 μg_{Pt} cm^{-2}, the surface area normalized borohydride oxidation currents under peaks **a1** and **a2** are ca. 1.6–1.8 and 1.9–2.5, respectively, times higher on the latter catalyst (Fig. 5b, b'). The analysis of the data in Fig. 5c, c' clearly points to the fact that Pt mass currents of the Pt/TiO_2-NTs catalyst with the Pt loading of 16.3 μg_{Pt} cm^{-2} are ca. 2.8–4.0 times greater under peak **a1** and ca. 4–6 greater under peak **a2** also than compared to those of the Pt/TiO_2-NTs catalysts with higher Pt loadings of 88.9 and 219.0 μg_{Pt} cm^{-2}, respectively.

The comparison of the data, obtained after normalization to the ECSAs with those calculated for the geometric area ones, shows that the trends of borohydride anodic oxidation depends on the size and structure of Pt particles in a rather complex and complicated manner (cf. Fig. 5a, b). Generally, small Pt particles of 10–50 nm are most active and provide the highest borohydride oxidation parameters. Recent electrochemical studies [43, 44] suggest that the borohydride oxidation reaction is subjected to a lot of factors such as nanoparticles size, inter-particle distance, loading, thickness of the active layer, etc. Bearing in mind that the dissociative adsorption of BH_4^- over the Pt surface is highly favourable at all potentials of interest (including open circuit potential) and requires nine free neighbouring Pt sites to proceed [39], the aforementioned factors are essential. Too small nanoparticles cannot provide enough surface area for the reaction, conversely to what happens on larger nanoparticles. A larger particle diameter and a shorter inter-particle distance yield a faster BOR kinetics and a larger faradaic efficiency. On the other hand, the thick volumic active layers contain numerous sites for the reaction to proceed, but these sites remain insufficiently fed by a "fresh" $NaBH_4$ solution, since the layer feeding operates only from the top of the surface [44], i.e. thick layers undergo a great diffusion limitation of BH_4^- species within their thickness, resulting in a low effectiveness factor of the Pt sites. Moreover, it should be taken into account that Pt surfaces are sensitive to surface poisoning and deactivation by either the final products of the BOR (BO_x) and/or their intermediates ($BH_{x,ad}$ species). The FTIR data obtained for Pt electrodes [45] clearly direct toward the detrimental effect of the surface blocking by $BH_{2,ad}$ species, which were detected at low potentials and seemed to accumulate at the Pt|electrolyte interface at low potentials. Therefore the residence time of those moieties at the surface also matters, particularly in static, i.e. natural diffusion conditions. It is obvious that the structure/morphology of the surface affects the rate of BOR in a rather complicated way with a lot of factors to be considered. Taken together these observations points to the fact that the Pt/TiO_2-NTs catalyst with the Pt loading of 16.3 μg_{Pt} cm^{-2} and with deposited Pt nanoparticles in the range ca. from a few to 50 nm in size has the highest specific and mass activity for the oxidation of BH_4^- ions. The determined activity can possibly be related to the production of smaller Pt nanoparticles, as well as their fine and relatively uniform dispersion on the TiO_2-NTs.

CONCLUSIONS

In this study we have successfully prepared the Pt/TiO_2-NTs catalysts with different Pt loadings equal to 16.3, 88.9 and 219.0 μg_{Pt} cm^{-2}, by a simple direct electrodeposition of Pt nanoparticles onto the TiO_2-NTs arrays from the platinum-containing solution. It has been determined that the size of Pt crystallites deposited onto the TiO_2-NTs surfaces ranged from ca. a few to 50 or even more nm in size depending upon the Pt deposition time applied.

The Pt/TiO_2-NTs catalysts prepared with higher Pt loadings of 88.9 and 219.0 had considerably higher ECSAs and demonstrated significantly higher anodic currents towards the oxidation of H_2 generated by both the catalytic hydrolysis of BH_4^- and oxidation of BH_4^- ions as compared to those of the smooth Pt.

The Pt/TiO_2-NTs catalyst with the Pt loading of 16.3 μg_{Pt} cm^{-2} and with the deposited Pt nanoparticles in the range ca. from a few to 50 nm in size has the highest specific and mass activities for the oxidation of BH_4^- ions. The fabricated Pt/TiO_2-NTs electrodes seem to be a promising anodic material for direct borohydride fuel cells.

Received 24 July 2017
Accepted 4 October 2017

References

1. D. M. F. Santos, C. A. C. Sequeira, *Renew. Sust. Energy Rev.*, **15**, 3980 (2011).
2. J.-H. Wee, *J. Power Sources*, **155**, 329 (2006).
3. C. Ponce de Leon, F. C. Walsh, D. Pletcher, D. J. Browning, J. B. Lakeman, *J. Power Sources*, **155**, 172 (2006).
4. J. Ma, N. A. Choudhury, Y. Sahai, *Renew. Sust. Energy Rev.*, **14**, 183 (2010).
5. M.-H. Wee, *J. Power Sources*, **161**, 1 (2006).
6. L. Yi, Y. Song, X. Liu, X. Wang, G. Zou, P. He, W. Yi, *Int. J. Hydrogen Energy*, **36**, 15775 (2011).
7. S. Li, L. Wang, J. Chu, H. Zhu, Y. Chen, Y. Liu, *Int. J. Hydrogen Energy*, **41**, 8583 (2016).
8. Z. Sukackienė, L. Tamašauskaitė-Tamašiūnaitė, A. Balčiūnaitė, et al., *J. Electrochem. Soc.*, **162**, 734 (2015).
9. L. Tamašauskaitė-Tamašiūnaitė, A. Jagminienė, A. Balčiūnaitė, et al., *Int. J. Hydrogen Energy*, **38**, 14232 (2013).
10. L. Yi, W. Wei, C. Zhao, L. Tian, J. Liu, X. Wang, *J. Power Sources*, **285**, 325 (2015).

11. D. Duan, J. Liang, H. Liu, et al., *Int. J. Hydrogen Energy*, **40**, 488 (2015).
12. L. Tamašauskaitė-Tamašiūnaitė, A. Balčiūnaitė, D. Šimkūnaitė, A. Selskis, *J. Power Sources*, **202**, 85 (2012).
13. L. Tamašauskaitė-Tamašiūnaitė, A. Balčiūnaitė, R. Čekavičiūtė, A. Selskis, *J. Electrochem. Soc*., **159**, B611 (2012).
14. P. He, X. Wang, P. Fu, H. Wang, L. Yi, *Int. J. Hydrogen Energy*, **36**, 8857 (2011).
15. D. Duan, H. Liu, X. You, H. Wei, S. Liu, *J. Power Sources*, **293**, 292 (2015).
16. L. Jing, Q. Zhao, S. Chen, L. Yi, X. Wang, W. Wei, *Electrochim. Acta*, **171**, 96 (2015).
17. A. Balčiūnaitė, Z. Sukackienė, L. Tamašauskaitė-Tamašiūnaitė, Ž. Činčienė, A. Selskis, E. Norkus, *Electrochim. Acta*, **225**, 255 (2017).
18. L. Yi, L. Liu, X. Liu, et al., *Int. J. Hydrogen Energy*, **37**, 12650 (2012).
19. B. Šljukić, J. Milikić, D. M. F. Santos, C. A. C. Sequeira, *Electrochim. Acta*, **107**, 577 (2013).
20. L. Yi, W. Wei, C. Zhao, et al., *Electrochim. Acta*, **158**, 209 (2015).
21. J. Liu, L. Yi, X. Wang, et al., *Int. J. Hydrogen Energy*, **40**, 7301 (2015).
22. M. G. Hosseini, M. Abdolmaleki, F. Nasirpouri, *Electrochim. Acta*, **114**, 215, (2013).
23. J. Nian, H. Teng, *J. Phys. Chem. B*, **110**, 4193 (2006).
24. Y. Lan, X. Gao, H. Zhu, et al., *Adv. Funct. Mater.*, **15**, 1310 (2005).
25. F. Amano, T. Yasumoto, T. Shibayama, S. Uchida, B. Ohtani, Appl. Catal. B, **89**, 583 (2009).
26. P. Benvenuto, A. K. M. Kafi, A. Chen, *J. Electroanal. Chem*., **627**, 76 (2009).
27. V. Idakiev, Z. Y. Yuan, T. Tabakova, B. L. Su, *Appl. Catal*., A **281**, 149 (2005).
28. Q. Zhao, M. Li, J. Chu, T. Jiang, H. Yin, *Appl. Surf. Sci*., **255**, 3773 (2009).
29. L. M. Roen, C. H. Paik, T. D. Jarvic, *Electrochem. Solid St*., **7**, A19 (2004).
30. S. Trasatti, O. A. Petrii, *Pure Appl. Chem.*, **63**, 711 (1991).
31. L. Tamašauskaitė-Tamašūnaitė, A. Balčiūnaitė, A. Zabielaitė, et al., *J. Electroanal. Chem*., **707**, 31 (2013).
32. D. A. Finkelstein, N. D. Mota, J. L. Cohen, H. D. Abruna, *J. Phys. Chem. C*, **113**, 19700 (2009).
33. E. Gyenge, *Electrochim. Acta*, **49**, 965 (2004).
34. V. W. S. Lam, D. C. W. Kannangara, A. Alfantazi, E. L. Gyenge, *J. Phys. Chem. C*., **115**, 2727 (2011).
35. B. H. Liu, Z. P. Li, S. Suda, *Electrochim. Acta*, **49**, 3097 (2004).
36. E. Gyenge, M. Atwan, D. Northwood, *J. Electrochem. Soc*., **153**, A150, (2006).
37. L. C. Nagle, J. F. Rohan, *J. Electrochem. Soc*., **153**, C773 (2006).
38. B. H. Liu, Z. P. Li, S. Suda, *Electrochim. Acta*, **49**, 3097 (2004).
39. G. Rostamikia, M. J. Janik, *Electrochim. Acta*, **55**, 1175 (2010).
40. R. Jamard, A. Latour, J. Salomon, Ph. Capron, A. Martinent-Beaumont, *J. Power Sources*, **176**, 287 (2008).
41. C. Celik, F. G. B. San, H. I. Sarac, *J. Power Sources*, **195**, 2599 (2010).
42. Y.-B. He, G.-R. Li, Z.-L. Wang, Y.-N. Ou, Y.-X. Tog, *J. Phys. Chem. C*., **114**, 19175 (2010).
43. K. S. Freitas, B. M. Concha, E. A. Ticianelli, M. Chatenet, *Catal. Today*, **170**, 110 (2011).
44. P.-Y. Olu, C. Barros, N. Job, M. Chatenet, *Electrocatal*. **5**, 288 (2014).
45. B. Molina Concha, M. Chatenet, E. A. Ticianelli, F. H. B. Lima, *J. Phys. Chem. C.*, **115**, 12439 (2011).

Dijana Šimkūnaitė, Loreta Tamašauskaitė-Tamašiūnaitė, Aldona Balčiūnaitė, Aušrinė Zabielaitė, Sigitas Jankauskas, Algirdas Selskis

PLATINOS / TITANO OKSIDO NANOVAMZDELIŲ ELETROKATALIZATORIAI BOROHIDRIDO OKSIDACIJAI

S a n t r a u k a

Darbe platinos / titano oksido nanovamzdelių (Pt/TiO_2-NV) katalizatoriai formuoti taikant elektrocheminio metalų nusodinimo metodą. Pt dalelės buvo elektronusodinamos tiesiogiai ant TiO_2-NV paviršiaus iš 1 mM H_2PtCl_6 + 0.1 M HCl 25°C temperatūros tirpalo, taikant 10 mA cm^{-2} srovės stiprumą 3, 15 ar 30 min. Gautų katalizatorių paviršiaus morfologija bei struktūra tirti lauko emisijos skenuojančios elektroninės mikroskopijos ir rentgeno spindulių energijos dispersinės analizės metodais. Pt/TiO_2-NV katalizatorių elektrokatalizinis aktyvumas natrio borohidrido oksidacijos reakcijai šarminėje terpėje tirtas taikant ciklinę voltamperometriją.

Taikant metalų elektrocheminio nusodinimo metodą, buvo suformuoti Pt/TiO_2-NV katalizatoriai, turintys skirtingą nusodintos Pt įkrovą – 16,3, 88,1 ir 219,0 μg_{Pt} cm^{-2}, o nusodintų Pt kristalitų dydis kito nuo kelių iki 50 nm, atskirais atvejais ir daugiau, priklausomai nuo Pt elektronusodinimo ant TiO_2-NV paviršiaus trukmės. Nustatyta, kad didžiausiu specifiniu ir masės kataliziniu aktyvumu natrio borohidrido oksidacijos reakcijai pasižymėjo Pt/TiO_2-NV katalizatoriai, kai nusodintų Pt dalelių dydis buvo 10–50 nm, o nusodintos Pt įkrova – 16,3 μg_{Pt} cm^{-2}.